

MRI-directed cognitive fusion-guided biopsy of the anterior prostate tumors

Ian G. Murphy
Elaine NiMhurchu
Robert G. Gibney
Colm J. McMahon

PURPOSE

We aimed to evaluate the efficacy of magnetic resonance imaging (MRI)-directed cognitive fusion transrectal ultrasonography (TRUS)-guided anterior prostate biopsy for diagnosis of anterior prostate tumors and to illustrate this technique.

METHODS

A total of 39 patients with previous negative TRUS biopsy, but high clinical suspicion of occult prostate cancer, prospectively underwent prostate MRI including diffusion-weighted imaging (DWI). Patients with a suspicious anterior lesion on MRI underwent targeted anterior gland TRUS-guided biopsy with cognitive fusion technique using sagittal probe orientation. PIRADS version 1 scores (T2, DWI, and overall), lesion size, prostate-specific antigen (PSA), PSA density, and prostate gland volume were compared between positive and negative biopsy groups and between clinically significant cancer and remaining cases. Logistic regression analysis of imaging parameters and prostate cancer diagnosis was performed.

RESULTS

Anterior gland prostate adenocarcinoma was diagnosed in 18 patients (46.2%) on targeted anterior gland TRUS-guided biopsy. Clinically significant prostate cancer was diagnosed in 13 patients (33.3%). MRI lesion size, T2, DWI, and overall PIRADS scores were significantly higher in patients with positive targeted biopsies and those with clinically significant cancer ($P < 0.05$). Biopsies were positive in 90%, 33%, and 29% of patients with overall PIRADS scores of 5, 4, and 3 respectively. Overall PIRADS score was an independent predictor of all prostate cancer diagnosis and of clinically significant prostate cancer diagnosis.

CONCLUSION

Targeted anterior gland TRUS-guided biopsy with MRI-directed cognitive fusion enables accurate sampling and may improve tumor detection yield of anterior prostate cancer.

Patients with clinical suspicion of malignant prostate neoplasm (i.e., elevated prostate-specific antigen [PSA], suspicious nodule on digital rectal examination) typically undergo systematic transrectal ultrasonography (TRUS)-guided sectoral biopsy; however, the overall yield of initial biopsy is 22%–29% (1, 2). Potential reasons for false negative TRUS biopsy include sampling error or technical limitation due to the location of tumor. Anteriorly located tumors, where the dominant tumor mass is anterior to the urethra represent a particular diagnostic challenge, as they are not sampled in standard systematic 12-core needle biopsy, and it is estimated that 21% of malignant prostate tumors occur in the anterior prostate (3, 4). Furthermore, when TRUS biopsy detects minimal volume/low-grade carcinoma, failure to sample a coexistent more aggressive anterior tumor may lead to an underestimation of disease burden and aggressiveness (5) and inappropriate management by enrollment in an active surveillance program.

In addition to an established role in the staging of prostate cancer (6–8), magnetic resonance imaging (MRI) has an increasing role for the localization of prostate tumors which can then be targeted for biopsy (9–11). For lesion localization, anatomic T2-weighted sequences are combined with one or more functional technique including diffusion-weighted imaging (DWI) (12), magnetic resonance spectroscopy (MRS) or dynamic contrast-enhanced (DCE) MRI (9–11). Based on suspicion of prostate cancer, targeted biopsy of the suspicious area can then be performed with either MRI guidance (10) or TRUS guidance. The level of suspicion of prostate cancer on MRI can be quantified using the Prostate Imaging Reporting and Data

From the Department of Radiology (I.G.M., E.N., R.G., C.J.M.) ✉ colmjcmahon@yahoo.co.uk St. Vincent's University Hospital, Dublin Ireland; the Department of Radiology (C.J.M.), Beth Israel Deaconess Medical Center, Boston, USA.

Received 23 September 2015; revision requested 13 April 2016; revision received 10 May 2016; accepted 25 May 2016.

Published online 11 January 2017.
DOI 10.5152/dir.2016.15445

System (PIRADS) (13). Where TRUS is used to guide targeted biopsy, electronic fusion of magnetic resonance images with TRUS images can be performed to guide biopsy (14, 15), or “cognitive fusion” can be used (16), by which the operator prospectively reviews the MRI appearances and uses TRUS to guide targeted sampling of the area of suspected tumor in the prostate gland.

Limited literature is available regarding the technique for TRUS-guided biopsy of the anterior apex of the prostate (17, 18). The goal of the current study is to evaluate the effectiveness of MRI-directed cognitive fusion TRUS-guided anterior prostate biopsy for diagnosis of anterior prostate tumors and to illustrate this technique.

Methods

Study design

The study was reviewed by the institutional ethics committee and approved as a clinical audit. In accordance with local policy, informed consent was not required. Patients were included if they had undergone MRI-directed targeted TRUS-guided anterior prostate biopsy in 2011–2014 because of suspicion of anterior tumor on MRI (Chart 1). All patients had undergone previous nontargeted TRUS-guided sectoral biopsy which was negative for carcinoma, but had undergone MRI for further evaluation due to persistent clinical concern for occult neoplasm.

MRI technique

All patients were scanned using 1.5 T MRI whole body scanner (GE Signa HDx or Siemens Avanto), with phased array external surface coil with biparametric technique (T2-weighted imaging and DWI) (19). MRI scan technique included multiplanar T2-weighted imaging including high-resolution axial T2-weighted images (TR, 3720 ms; TE, 107 ms; NEX, 4; slice thickness, 3 mm; interslice gap, 0 mm) and diffusion-weighted images (Siemens: TR, 4100; TE, 84 ms; NEX, 4; slice thickness, 4 mm; interslice gap, 0 mm; b

values, 50, 400, 800 s/mm²; GE: TR, 5000 ms; TE, minimum; NEX, 8; slice thickness, 3 mm; interslice gap, 1 mm; b value, 800 s/mm²).

MRI interpretation

For the purpose of this analysis, MRI findings of each patient were reviewed retrospectively by two radiologists with five and three years of experience in pelvic MRI interpretation. The studies were reviewed in a randomized order, with the radiologists blinded to the biopsy results. For each patient the anterior lesion suspected on MRI, which had prompted targeted biopsy, was scored using the PIRADS system (version 1) (13), with scores ranging 1–5 for T2 and DWI appearances. Interpretation of DWI data included both diffusion-weighted images and apparent diffusion coefficient (ADC) map, which were analyzed qualitatively. An overall score was also applied based on overall interpretation of MRI findings and scored 1–5. Additionally, the maximum dimension of the lesion on MRI was measured on the axial T2-weighted images, while visually referencing the diffusion-weighted images and ADC map. Two radiologists in consensus carried out all scoring and measurements. The overall prostate volume was calculated by multiplying the maximum dimensions of the gland in three planes (anterior-to-posterior × transverse × craniocaudal) × 0.52.

Anterior TRUS biopsy technique

All biopsies were performed using either a BK ProFocus 2202 ultrasound machine (BK Medical) with the end-fire convex array of a multi-frequency 8818 transducer or a Phillips iU22 ultrasound machine (Philips Healthcare), with an end-fire curved array C9-5ec transducer. All biopsies were performed by one of two radiologists with seven and 30 years of experience in TRUS prostate biopsy. At our institution, TRUS biopsies (both standard systematic and targeted) are typically performed with conscious sedation, peri-prostatic local anesthetic (10 mL 1% lidocaine) and a transverse plane of US and biopsy guidance. This limits effective sampling of the anterior gland. In a modification of technique described for apical anterior horn biopsy (17, 18), a sagittal plane of TRUS imaging and biopsy guidance was used. The endorectal ultrasound probe was positioned in the sagittal plane, such that the needle guide was positioned anteriorly with respect to the probe (Fig. 2). Cognitive fusion was employed to determine the exact location of biopsy sampling, following review of the

patient’s MRI. The probe was then angled as needed in the sagittal plane such that the needle trajectory included the area of concern (Fig. 1). For lesions located more cranially, the biopsy needle was advanced 1–2 cm into the prostate gland prior to deploying the biopsy device. For more caudally located lesions, the biopsy device was activated from the prostate surface or with minimal advancement into the gland prior to triggering the device. Medial-to-lateral localization was performed by identifying the urethra in the midline as a landmark, then scanning laterally to the lateral margin of the gland to define the lateral border. Samples were taken more medially or laterally as needed based on the preprocedure MRI. Finally, if a concordant hypoechoic nodule was identified in a similar position to a suspicious lesion on MRI, the biopsy needle was directed into this area. At least two cores of tissue were obtained from the target area.

Clinical and biopsy data

Patient age and PSA levels prior to biopsy were recorded. PSA density was calculated by dividing serum PSA by prostate gland volume as determined on MRI. Gleason grade of biopsy samples positive for carcinoma were recorded in addition to the percentage of core biopsy sample involved by tumor. Clinically significant cancers were defined based on Epstein criteria: Gleason grade of ≥7; or percentage core biopsy involvement by tumor ≥50% (20, 21).

Statistical analysis

All analysis was performed using STATA Version 13.1 (Statacorp).

The primary hypothesis was that targeted anterior prostate biopsy would have a similar yield to that established in the existing literature for targeted prostate biopsy not limited to the anterior prostate gland. The yield of targeted TRUS biopsy based on MRI findings for the diagnosis of occult prostate cancer ranges from 39%–56% (10, 12, 16, 22, 23). For the purpose of sample size calculation, the null hypothesis was that the yield of anterior biopsy would be low (20%) and the alternative hypothesis was that the yield would be similar to the literature for targeted prostate biopsy not limited to the anterior prostate gland (45%). Sample size estimation was carried out using power analysis for a one sample Wald test with probability (power) of 0.9, and type I error probability of 0.05. This resulted in sample size estimation of 42.

Main points

- Transrectal targeted ultrasound-guided biopsy with cognitive fusion allows accurate sampling of clinically significant anterior prostate tumors suspected on MRI.
- In this setting, overall PIRADS score was an independent predictor of positive biopsy.
- PSA density was higher in those with positive biopsies; however, PSA was not.

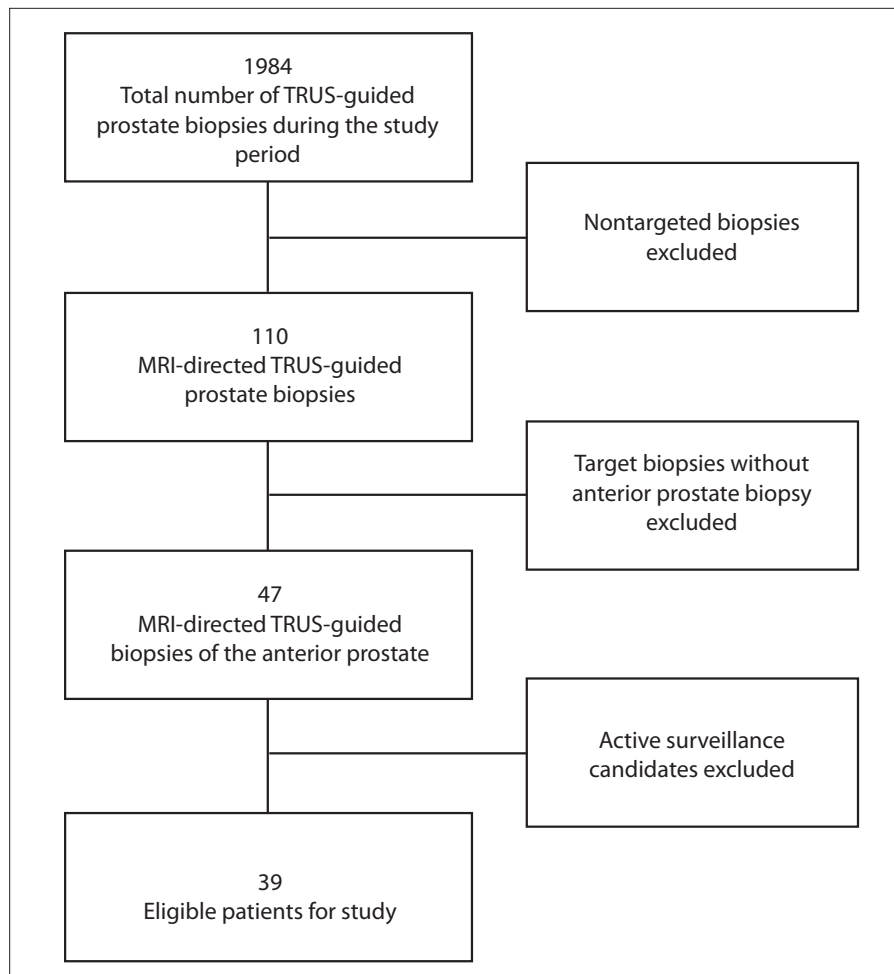


Figure 1. Flowchart demonstrating subject selection TRUS, transrectal ultrasonography; MRI, magnetic resonance imaging.

Table 1. Baseline characteristics of study population	
Patients (n)	39
Age (years), mean±SD	67.1±7.6
PSA (ng/mL), mean±SD	15.2±9.3
Prostate volume (cc), mean±SD	71.4±36.2
PSA density (ng/mL per cc of prostate volume), mean ±SD	0.25±0.17
Anterior lesion size on MRI (mm), mean±SD	16.5±7.7
Overall PIRADS score, n/N (%)	
3	14/39 (35.9)
4	15/39 (38.5)
5	10/39 (25.6)

SD, standard deviation; PSA, prostate-specific antigen; MRI, magnetic resonance imaging; PIRADS, prostate imaging reporting and data system.

The mean (±standard deviation) patient age, PSA, prostate volume, PSA density, lesion size, and PIRADS scores for all patients were calculated.

PIRADS scores (overall score, T2 score, DWI score) were compared between positive

and negative biopsy groups using a Mann-Whitney U test. In a similar way, PIRADS scores were also compared between cases where clinically significant cancer was diagnosed and the remaining cases (negative and clinically insignificant cancer).

Continuous data (age, lesion size, PSA, prostate volume, PSA density) were compared between biopsy positive and negative groups using an independent samples t-test. In a similar way, continuous data were compared between clinically significant cancer cases and the remaining cases.

The positive predictive value of PIRADS overall score for prediction of a positive targeted biopsy and for the prediction of clinically significant cancer was calculated. Forward stepwise logistic regression analysis was performed for prediction of positive biopsy and for prediction of clinically significant cancer diagnosis.

Results

During the study period, 1984 TRUS-guided prostate biopsies were performed at this institution. Of these, 110 were targeted biopsies with MRI-directed cognitive fusion technique. Of these, 47 cases had biopsy targeted to an anterior prostate lesion. Excluding patients with previous positive biopsy (active surveillance candidates), 39 patients were eligible for the study. Mean age was 67.1±7.6 years. Case examples are shown in Figs. 3 and 4. Patient demographics, imaging and biochemical parameters are presented in Table 1.

Comparison of overall biopsy yield with PIRADS score, lesion size, PSA, prostate volume, and PSA density is presented in Table 2. Comparison of clinically significant prostate cancer yield with PIRADS score, lesion size, PSA, prostate volume, and PSA density is presented in Table 3. The overall PIRADS score, T2 score and DWI score were all significantly higher in the positive biopsy group compared with the negative biopsy group, and were also higher in cases of clinically significant cancer diagnosis. Serum PSA was not significantly different between positive and negative biopsy groups or between clinically significant cancer and remaining cases. However, PSA density was higher in patients with positive biopsies. Forward stepwise logistic regression analysis demonstrated that overall PIRADS score was an independent predictive factor for positive biopsy (odds ratio, 3.77; 95% confidence interval [CI], 1.40–10.16; $P = 0.009$) and for the diagnosis of clinically significant cancer (odds ratio, 3.91; 95% CI, 1.38–11.09; $P = 0.011$).

The positive predictive values of overall PIRADS 3, 4, and 5 score for positive anterior targeted biopsy were 29%, 33%, and 90%, respectively, and for clinically significant cancer were 21%, 13%, and 80%, respectively.

Table 2. Comparison of MRI and PSA parameters with biopsy results

	Positive biopsy	Negative biopsy	<i>P</i>
Patients, n/N (%)	18/39 (46.15)	21/39 (53.85)	
Target lesion size (mm) ^a	20.2 (15.9–24.5)	13.4 (11.0–15.8)	0.005
Overall PIRADS score ^b	4.5 (4–5)	4 (3–4)	0.007
T2 PIRADS score ^b	4 (3–4)	3 (3–4)	0.027
DWI PIRADS score ^b	5 (5–5)	4 (4–5)	0.023
PSA (ng/mL) ^a	16.3 (10.6–22.0)	14.1 (10.9–17.4)	0.470
Prostate volume (cc) ^a	54.8 (43.5–66.1)	85.6 (67.5–103.8)	0.006
PSA density (ng/mL per cc of prostate volume) ^a	0.313 (0.211–0.414)	0.191 (0.139–0.244)	0.025

P < 0.05 was used as threshold for significance.

MRI, magnetic resonance imaging; PSA, prostate-specific antigen; PIRADS, prostate imaging reporting and data system; DWI, diffusion-weighted imaging.

^aMean (95% confidence interval); ^bMedian (interquartile range).

Table 3. Comparison of MRI and PSA parameters with clinically significant cancer results

	Clinically significant cancer	Negative biopsy or clinically insignificant cancer	<i>P</i>
Patients, n/N (%)	13/39 (33.3)	26/39 (66.7)	
Target lesion size (mm) ^a	20.5 (14.4–26.5)	14.6 (12.3–16.8)	0.023
Overall PIRADS score ^b	5 (4–5)	4 (3–4)	0.009
T2 PIRADS score ^b	4 (4–4)	3 (3–4)	0.039
DWI PIRADS score ^b	5 (5–5)	4.5 (4–5)	0.095
PSA (ng/mL) ^a	18.3 (10.8–25.8)	13.6 (10.7–16.5)	0.139
Prostate volume (cc) ^a	59.2 (44.2–74.1)	77.5 (31.4–93.6)	0.138
PSA density (ng/mL per cc of prostate volume) ^a	0.309 (0.211–0.408)	0.217 (0.148–0.285)	0.112

P < 0.05 was used as threshold for significance.

MRI, magnetic resonance imaging; PSA, prostate-specific antigen; PIRADS, prostate imaging reporting and data system; DWI, diffusion-weighted imaging.

^aMean (95% confidence interval); ^bMedian (interquartile range).

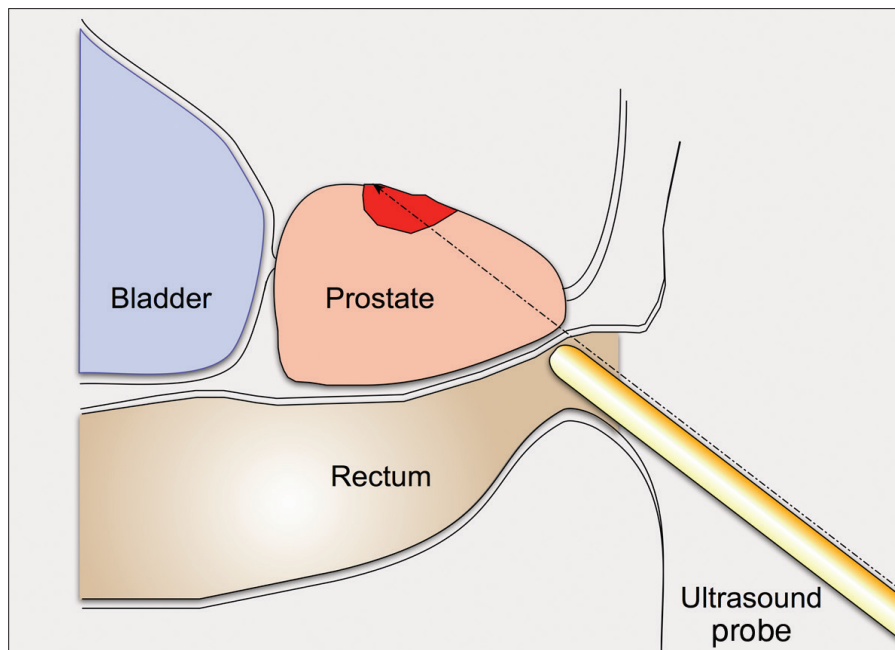


Figure 2. Schematic illustration of targeted anterior biopsy technique. The transducer is positioned in sagittal orientation with needle path to anterior gland tumor shown as a dashed line.

ly. Biopsies were more likely to be positive in larger lesions; the mean maximum diameter of lesions on MRI with subsequent positive biopsy was 20.2±8.7 mm vs. 13.4±5.3 mm for cases with negative biopsy (*P* = 0.005).

In 18 of 39 patients (46.2%), adenocarcinoma was identified in the anterior targeted biopsy samples. Clinically significant cancer was identified in 13 of 39 patients (33.3%). The mean age was 68.1±8.6 years in patients with positive targeted biopsy, and 66.1±6.7 years in those with negative biopsy.

On histology, the overall median tumor Gleason grade was 7 (range, 6–9). Six cases had Gleason 6 (3+3) tumors. Nine cases had Gleason 7 tumors, of which there were eight (3+4) and two (4+3) cases. There were three Gleason 9 (4+5) tumors. The mean percentage of involvement by tumor of each core sample was 30.6%±21.2%.

Review of microbiology records for positive urine cultures within one week following the biopsy date, and the radiology information system for complications revealed one case of postprocedural sepsis. The patient was successfully treated with intravenous antibiotics for five days (gentamycin and amoxicillin-clavulanate), with a subsequent course of oral antibiotics and sepsis resolved without long-term consequences.

Discussion

In this study, a technically feasible transrectal approach to targeting anterior prostate lesions identified with MRI for biopsy is described and validated by correlating results with MRI PIRADS score. The results indicate a close correlation of targeted biopsy results with PIRADS overall score, with 90% of biopsies positive in cases with the highest prebiopsy suspicion based on MRI PIRADS 5 score. The yield was moderate in cases with PIRADS 4 (33%) and PIRADS 3 (29%) lesions.

These targeted anterior biopsy results, with an overall yield of 46.2%, compare favorably with the existing literature for MRI-directed TRUS prostate biopsies for biopsy-occult tumors in other parts of the prostate (not confined to the anterior prostate), where cancer diagnosis ranges from 39% to 56% (10, 12, 16, 22, 23). For example, using a cognitive fusion technique, Park et al. (12) demonstrated an overall yield of 39.5% of prostate cancer in a study of 43 men with prior negative biopsy, persistent elevation of PSA, and suspicious lesion on MRI. MRI has been shown to correlate with anterior biopsy findings, but previous studies have used positive anterior biopsy as a starting point,

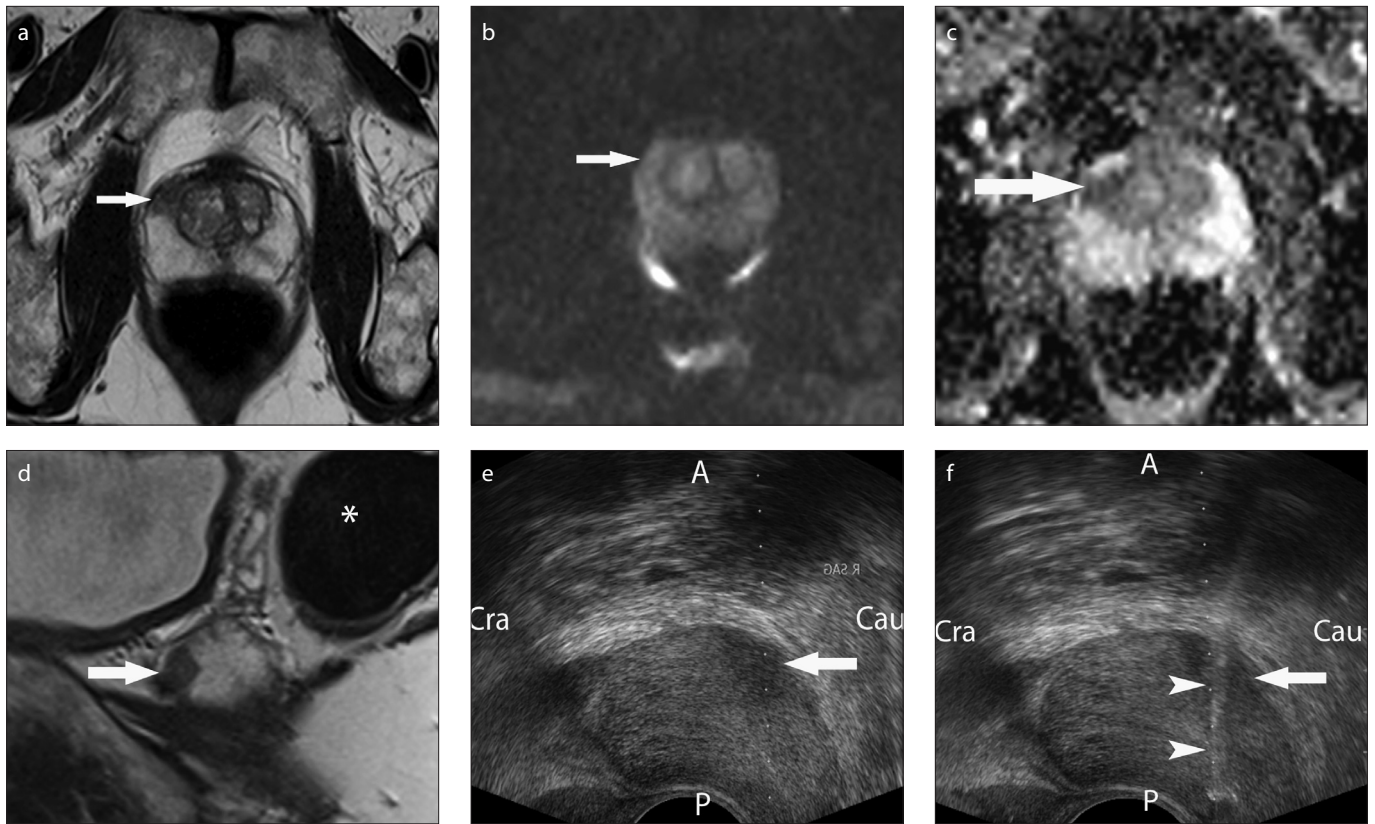


Figure 3. a–f. A 63-year-old man considering active surveillance for minimal volume low-grade prostate cancer. Initial sectoral biopsy was positive for Gleason grade 6 carcinoma, in two cores with 5% and <5% of core length involved in these samples. Axial T2-weighted image (a) demonstrates an anterior lesion centered in the right mid anterior peripheral zone (arrow); T2 PIRADS score was 4. Axial $b=800 \text{ s/mm}^2$ DWI (b) demonstrates isointensity of the lesion (arrow). Axial ADC map (c) shows an area of restricted diffusion correlating with T2 appearance; DWI PIRADS score was 4. Sagittal T2-weighted image (d) demonstrates the same lesion as a wedge-shaped anterior low-signal lesion (arrow). Note rectum posteriorly (asterisk). TRUS (e) with sagittal probe orientation; in this case a matching hypoechoic lesion is seen anteriorly (arrow). Anterior, posterior, caudal, and cranial orientations are denoted by A, P, Cau, and Cra, respectively. Targeted anterior TRUS-guided biopsy image (f) demonstrates an 18 G biopsy needle (arrowheads) in the mass (arrow) and yielded diagnostic samples. Overall PIRADS score was 4. Targeted anterior biopsy yielded 50% of core length samples positive for Gleason grade 7 prostate carcinoma. Radical prostatectomy was performed, and the anterior gland lesion was confirmed as a gland-confined Gleason grade 7 carcinoma.

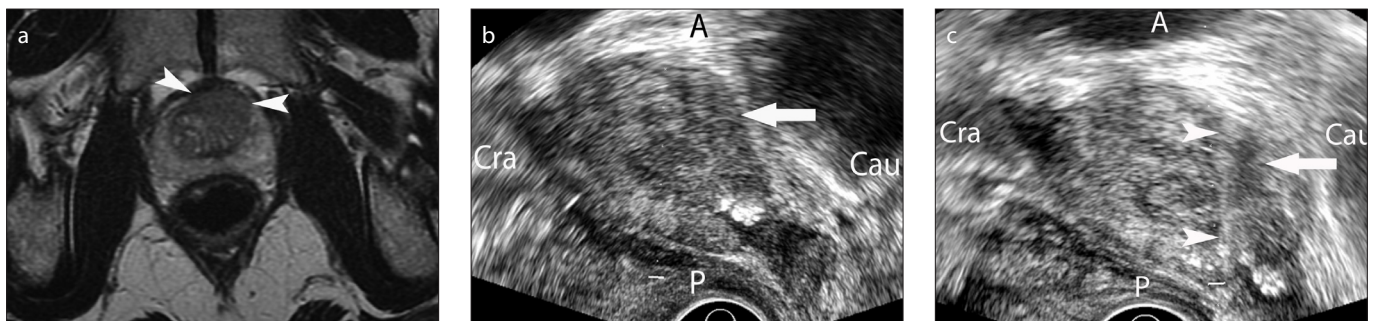


Figure 4. a–c. A 51-year-old man with previous negative TRUS biopsy. Rising PSA prompted MRI and subsequent targeted anterior TRUS biopsy. Axial T2-weighted image (a) demonstrates anterior low signal mass (arrowheads), with ill-defined borders (“erased charcoal sign”) invading anterior fibromuscular stroma; T2W PIRADS score was 5. On sagittal TRUS image (b), the mass is visualized as a hypoechoic lesion along the anterior prostate (arrow). Anterior, posterior, caudal, and cranial orientations are denoted by A, P, Cau, and Cra, respectively. Targeted anterior TRUS-guided biopsy image (c) shows the 18 G biopsy needle (arrowheads) sampling the anterior gland lesion (arrow). Overall PIRADS was designated as 5. Targeted biopsy samples diagnosed Gleason grade 7 prostate carcinoma.

with MRI findings analyzed retrospectively (5, 24). The current study, however, includes all cases where an anterior targeted biopsy was performed based on MRI suspicion of prostate cancer (PIRADS 3 or greater).

The advantage of the technique utilized in this study is the use of widely available TRUS

equipment and procedure performance with conscious sedation and local anesthetic. The results of the current study also compare favorably with the efficacy of transperineal template biopsy. For example, Taira et al. (25) demonstrated a yield of 47% of prostate cancer in men with previous nega-

tive biopsy, with a high prevalence of occult anterior tumors diagnosed in that study, although results were not limited to anterior lesions. Additional alternative approaches include MRI-guided (in-bore) biopsies (26); however, the hardware and expertise for this approach is less widely available than

for TRUS biopsy. Saturation biopsies can also be performed in the setting of clinical suspicion of biopsy-occult prostate cancer (27) but require a high number of biopsy passes, without specifically targeting the areas of potentially highest yield. Another promising technique is electronic fusion of magnetic resonance and TRUS images to guide biopsy. With this technique, software is used to coregister prior MRI data and real-time TRUS images (14). This makes use of spatial positioning sensors attached to the endorectal ultrasound probe. Images from the MRI are reconstructed to the real-time plane of TRUS imaging thereby providing increased certainty that the TRUS-guided biopsy is effectively sampling the area of concern on MRI (15).

Our study has some limitations. The study is a retrospective review. The MRI protocol included DWI in addition to anatomic imaging, a strategy that has been correlated with a high cancer detection rate particularly for high Gleason grade disease (28). However, the addition of a further functional sequence (DCE or MRS) may have refined the overall PIRADS score, with potential effect on correlation with biopsy result. It is noted that a b value of 800 s/mm² was used in this study. Higher b value imaging may be advantageous, where adequate signal-to-noise ratio (SNR) permits, as recommended by the PIRADS version 2 guidelines (29). Additionally, the use of a cognitive targeting technique to direct the biopsy makes it less certain that the exact location of the abnormality characterized on MRI has been sampled. The finding that the average size of lesions, which were positive for carcinoma on targeted biopsy was greater than those which were negative (20.2 mm vs. 13.4 mm) highlights this potential sampling limitation. However, it is interesting that such large lesions were present in patients with prior negative biopsies, highlighting the importance of strategies for diagnosis of occult anterior prostate tumors. Since the study group did not all have radical prostatectomy, we cannot determine the false negative biopsy rate in this study. It is also worth noting that the study does not include patients who had no target for biopsy in the anterior prostate gland, so the proportion of men with occult anterior tumors in the clinical settings described is not determined. A further consideration is the impact of operator experience on the efficacy of this technique. In the current study, the operators had experience in both prostate MRI and TRUS-guided biopsies

and an understanding of both modalities is needed to perform the procedure effectively. However, the transition from performing sectoral nontargeted biopsies to manipulating the biopsy needle into the portion of the gland deemed suspicious for neoplasm on MRI proved straightforward for both operators. It is noted that the targeted lesions were sometimes visible on ultrasound. However, this was not routinely documented, and the yield of visible lesions versus lesions that were sampled purely based on anatomic location could not be evaluated by this retrospective study.

All of the targeted anterior biopsies in this study were performed with a sagittal approach, described in detail above. It is hoped that this will be useful to the reader, as the exact biopsy technique for TRUS-guided targeted biopsy is often not specifically described in existing literature and this can be a barrier to implementing this approach in local clinical practice. This biopsy technique was well tolerated by all patients. The specific yield of targeted anterior biopsy with sagittal approach compared with axial approach was not directly compared in this study. In smaller volume prostate glands, based on local experience, some anterior tumors can be sampled using a transaxial approach. However, it is difficult to direct the biopsy needle into the anterior-most aspect of the prostate with axial TRUS imaging guidance in larger glands. We did not routinely perform both techniques, as performing both in all cases would have resulted in unnecessary additional biopsy passes.

In general terms, targeted prostate biopsy has a number of potential advantages. The morbidity associated with prostate biopsy, particularly procedure related sepsis has been shown to be related to the number of biopsy samples performed (30). In a study of 5802 biopsies in 2002, 50% had hematospermia at three days, and 3.5% developed sepsis (31). Targeted TRUS biopsy of the prostate has the potential to reduce the number of cores required by reducing the need for repeated extended (12-core) biopsies and could potentially reduce the yield of clinically insignificant prostate cancers (32).

In conclusion, MRI-directed targeted TRUS-guided prostate biopsy with cognitive fusion enables accurate sampling of clinically significant prostate cancer in the anterior prostate, enabling improved tumor detection yield of lesions occult to routine sectoral biopsy.

Conflict of interest disclosure

The authors declared no conflicts of interest.

References

1. Roehl KA, Antenor JAV, Catalona WJ. Serial biopsy results in prostate cancer screening study. *J Urol* 2002; 167:2435–2439. [\[Crossref\]](#)
2. Djavan B, Ravery V, Zlotta A, et al. Prospective evaluation of prostate cancer detected on biopsies 1, 2, 3 and 4: when should we stop? *J Urol* 2001; 166:1679–1683. [\[Crossref\]](#)
3. Al-Ahmadie HA, Tickoo SK, Olgac S, et al. Anterior-predominant prostatic tumors: zone of origin and pathologic outcomes at radical prostatectomy. *Am J Surg Pathol* 2008; 32:229–235. [\[Crossref\]](#)
4. Bott SRJ, Young MPA, Kellett MJ, Parkinson MC, Contributors to the UCL Hospitals' Trust Radical Prostatectomy Database. Anterior prostate cancer: is it more difficult to diagnose? *BJU International* 2002; 89:886–889. [\[Crossref\]](#)
5. Lawrentschuk N, Haider MA, Daljeet N, et al. "Prostatic evasive anterior tumours": the role of magnetic resonance imaging. *BJU Int* 2010; 105:1231–1236. [\[Crossref\]](#)
6. Hoeks CMA, Barentsz JO, Hambrock T, et al. Prostate cancer: multiparametric MR imaging for detection, localization, and staging. *Radiology* 2011; 261:46–66. [\[Crossref\]](#)
7. Bloch BN, Furman-Haran E, Helbich TH, et al. Prostate cancer: accurate determination of extracapsular extension with high-spatial-resolution dynamic contrast-enhanced and T2-weighted MR imaging—initial results 1. *Radiology* 2007; 245:176–185. [\[Crossref\]](#)
8. Graser A, Heuck A, Sommer B, et al. Per-sextant localization and staging of prostate cancer: correlation of imaging findings with whole-mount step section histopathology. *AJR Am J Roentgenol* 2007; 188:84–90. [\[Crossref\]](#)
9. Prando A, Kurhanewicz J, Borges AP, Oliveira EM Jr, Figueiredo E. Prostatic biopsy directed with endorectal MR spectroscopic imaging findings in patients with elevated prostate specific antigen levels and prior negative biopsy findings: early experience 1. *Radiology* 2005; 236:903–910. [\[Crossref\]](#)
10. Franiel T, Stephan C, Erbersdobler A, et al. Areas suspicious for prostate cancer: MR-guided biopsy in patients with at least one transrectal US-guided biopsy with a negative finding—multiparametric MR imaging for detection and biopsy planning. *Radiology* 2011; 259:162–172. [\[Crossref\]](#)
11. Sciarra A, Panebianco V, Cicciariello M, et al. Value of magnetic resonance spectroscopy imaging and dynamic contrast-enhanced imaging for detecting prostate cancer foci in men with prior negative biopsy. *Clin Cancer Res* 2010; 16:1875–1883. [\[Crossref\]](#)
12. Park BK, Lee HM, Kim CK, Choi HY, Park JW. Lesion localization in patients with a previous negative transrectal ultrasound biopsy and persistently elevated prostate specific antigen level using diffusion-weighted imaging at three Tesla before rebiopsy. *Invest Radiol* 2008; 43:789–793. [\[Crossref\]](#)
13. Barentsz JO, Richenberg J, Clements R, et al. ESUR prostate MR guidelines 2012. *Eur Radiol* 2012; 22:746–757. [\[Crossref\]](#)
14. Singh AK, Kruecker J, Xu S, et al. Initial clinical experience with real-time transrectal ultrasonography-magnetic resonance imaging fusion-guided prostate biopsy. *BJU Int* 2008; 101:841–845. [\[Crossref\]](#)

15. Cool DW, Zhang X, Romagnoli C, Izawa JI, Romano WM, Fenster A. Evaluation of MRI-TRUS fusion versus cognitive registration accuracy for MRI-targeted, TRUS-guided prostate biopsy. *AJR Am J Roentgenol* 2015; 204:83–91. [\[Crossref\]](#)
16. Testa C, Schiavina R, Lodi R, et al. Accuracy of MRI/MRSI-based transrectal ultrasound biopsy in peripheral and transition zones of the prostate gland in patients with prior negative biopsy. *NMR Biomed* 2010; 23:1017–1026. [\[Crossref\]](#)
17. Moussa AS, Meshref A, Schoenfeld L, et al. Importance of additional “extreme” anterior apical needle biopsies in the initial detection of prostate cancer. *Urology* 2010; 75:1034–1039. [\[Crossref\]](#)
18. Meng MV, Franks JH, Presti JC Jr, Shinohara K. The utility of apical anterior horn biopsies in prostate cancer detection. *Urol Oncol* 2003; 21:361–365. [\[Crossref\]](#)
19. Radtke JP, Boxler S, Kuru TH, et al. Improved detection of anterior fibromuscular stroma and transition zone prostate cancer using biparametric and multiparametric MRI with MRI-targeted biopsy and MRI-US fusion guidance. *Prostate Cancer Prostatic Dis* 2015; 18:288–296. [\[Crossref\]](#)
20. Epstein JI, Walsh PC, Carmichael M, Brendler CB. Pathologic and clinical findings to predict tumor extent of nonpalpable (stage T1c) prostate cancer. *JAMA* 1994; 271:368–374. [\[Crossref\]](#)
21. Murphy G, Haider M, Ghai S, Sreeharsha B. The expanding role of MRI in prostate cancer. *AJR Am J Radiol* 2013; 201:1229–1238. [\[Crossref\]](#)
22. Portalez D, Rollin G, Leandri P, et al. Prospective comparison of T2w-MRI and dynamic-contrast-enhanced MRI, 3D-MR spectroscopic imaging or diffusion-weighted MRI in repeat TRUS-guided biopsies. *Eur Radiol* 2010; 20:2781–2790. [\[Crossref\]](#)
23. Anastasiadis AG, Lichy MP, Nagele U, et al. MRI-guided biopsy of the prostate increases diagnostic performance in men with elevated or increasing PSA levels after previous negative TRUS biopsies. *Eur Urol* 2006; 50:738–749. [\[Crossref\]](#)
24. Ouzzane A, Puech P, Lemaitre L, Leroy X, Neveux P. Combined multiparametric MRI and targeted biopsies improve anterior prostate cancer detection, staging, and grading. *Urology* 2011; 78:1356–1362. [\[Crossref\]](#)
25. Taira AV, Merrick GS, Galbreath RW, et al. Performance of transperineal template-guided mapping biopsy in detecting prostate cancer in the initial and repeat biopsy setting. *Pros Cancer Prostatic Dis* 2009; 13:71–77. [\[Crossref\]](#)
26. Pondman KM, Fütterer JJ, Haken ten B, et al. MR-guided biopsy of the prostate: an overview of techniques and a systematic review. *Eur Urol* 2008; 54:517–527. [\[Crossref\]](#)
27. Delongchamps NB, Haas GP. Saturation biopsies for prostate cancer: current uses and future prospects. *Nat Rev Urol* 2009; 6:645–652. [\[Crossref\]](#)
28. Watanabe Y, Terai A, Araki T, et al. Detection and localization of prostate cancer with the targeted biopsy strategy based on ADC map: a prospective large-scale cohort study. *J Magn Reson Imaging* 2012; 35:1414–1421. [\[Crossref\]](#)
29. American College of Radiology. MR Prostate Imaging Reporting and Data System version 2.0. Available at <http://www.acr.org/~media/ACR/Documents/PDF/QualitySafety/Resources/PIRADS/PIRADS%20V2.pdf>.
30. Rodríguez LV, Terris MK. Risks and complications of transrectal ultrasound guided prostate needle biopsy: a prospective study and review of the literature. *J Urol* 1998; 160:2115–2120. [\[Crossref\]](#)
31. Raaijmakers R, Kirkels WJ, Roobol MJ, Wildhagen MF, Schrder FH. Complication rates and risk factors of 5802 transrectal ultrasound-guided sextant biopsies of the prostate within a population-based screening program. *Urology* 2002; 60:826–830. [\[Crossref\]](#)
32. Moore CM, Robertson NL, Arsanious N, et al. Image-guided prostate biopsy using magnetic resonance imaging-derived targets: a systematic review. *Eur Urol* 2013; 63:125–140. [\[Crossref\]](#)